ONLINE SUPPLEMENTAL MATERIAL

Cell fixation and preservation for droplet-based single-cell transcriptomics

Jonathan Alles[1,#], Nikos Karaiskos[1,#], Samantha D. Praktiknjo[1,#], Stefanie Grosswendt[1], Philipp Wahle[2], Pierre-Louis Ruffault[3], Salah Ayoub[1], Luisa Schreyer[1], Anastasiya Boltengagen[1], Carmen Birchmeier[3], Robert Zinzen[2], Christine Kocks[1,*], and Nikolaus Rajewsky[1,*]

[1] Systems Biology of Gene Regulatory Elements, [2] Systems Biology of Neural Tissue Differentiation, Berlin Institute for Medical Systems Biology (BIMSB), [3] Developmental Biology/Signal Transduction, Max Delbrück Center for Molecular Medicine in the Helmholtz Association (MDC), 13125 Berlin, Germany

[#] Contributed equally

* Correspondence: christine.kocks@mdc-berlin.de; rajewsky@mdc-berlin.de

Suppl. Table S1 Top 50 marker genes expressed in 4 873 fixed, primary cells from *Drosophila* embryos.

Suppl. Tables S1 and S2 contain the top 50 marker genes per cluster, provided by Seurat's function findAllMarkers [16]. We additionally ordered them per cluster in decreasing log2-fold change (log2FC). The Log2FC was computed for a given gene by dividing its average normalized expression for a given cluster over the average normalized expression in the rest of the clusters and taking the logarithm of the fold change.

Suppl. Table S2 Top 50 marker genes expressed in 4 366 sorted, fixed cells from mouse hindbrain and cerebellum. Explanations see legend to Table S1.

Suppl. Fig. S1 Computational cell selection and RNA, cDNA library and cell quality. Related to Figure 2.

a Identification of cell barcodes associated with single-cell transcriptomes in a pool of amplified single-cell libraries. Drop-seq involves Poisson-limited dilution of cells implying that the great majority of beads (more than 95% under our Drop-seq conditions) is not exposed to cells, only to ambient RNA. To identify the cell barcodes associated with cellular transcriptomes, cell barcodes are plotted in decreasing order of reads against the cumulative fraction of reads. The inflection point (red line) indicates the number of cells; human-mouse cell doublets were removed computationally. Note that sample 'Fixed 1 week' has less cells, because only a fraction of barcoded beads was used for library preparation.

b A sub-set of cells from the experiment depicted in Fig. 2 (Live: 99 human, 44 mouse cells; Fixed: 253 human, 90 mouse cells) was sequenced at a higher median depth of ~104 106 and ~53 500 aligned reads per cell. Note that the live sample appears to have more genes/UMIs, because fewer cells were sequenced, resulting in more reads per cell.

c-e Bioanalyzer traces. c High quality RNA could be extracted from rehydrated cells that were fixed and stored for 20 weeks. RNA integrity number 10 (highest score).

d Fixation and storage does not change the fragment size distribution of Drop-seq cDNA libraries. Libraries were purified with 0.6x SPRI beads.

e Parallel control purification of the cDNA library "Fixed 3 weeks" with 0.6x (fragments above 500 bp; upper panel) or 1.8x SPRI beads (all fragments; lower panel) did not reveal a major peak corresponding to small molecular weight fragments indicative of low quality RNA input cells. SPRI, Solid Phase Reversible Immobilization beads.

f Plot depicting the percentage of reads mapping to non-mitochondrially encoded genes. Stressed or broken cells loose non-mitochondrially encoded mRNAs owing to cell leakage, while mRNAs from mitochondrially encoded genes become enriched in broken cells (14). Loss of cytoplasmic reads in methanol fixed cells was below 10%.

Fig. S2 Fixed cell samples can be stored for weeks to give reproducible results. Related to Fig. 2.

a, b Drop-seq of mixed human and mouse cells (50 cells/µl), corresponding to a biological replicate of the experiment shown in Figure 2. Libraries were sequenced to a median depth of ~142 400 (Fixed 1 week) or ~28 500 (Fixed 3 weeks) aligned reads per cell.

a Plots show the number of human and mouse transcripts (UMIs) associating with a cell (dot) identified as human- or mouse-specific (blue or red, respectively). Cells expressing less than 3500 UMIs are grey. Both Drop-seq experiments yielded single-cell transcriptomes that allowed clear species separation and a low % of cell doublets.

b Distribution and the median of the number of genes and transcripts (UMIs) detected per cell expressing more than 3500 UMIs.

c Gene expression levels from live and fixed cells correlate well. Pairwise correlations between bulk mRNAseq libraries (left) and Drop-seq single-cell experiments (right) for cells expressing more than 3500 UMIs. Non-single cell bulk mRNA-seq data are shown as reads per kilobase per million (RPKM). Drop-seq expression counts were converted to average transcripts per million (ATPM) and plotted as log2 (ATPM + 1). Upper right panel depicts Pearson correlations. The intersection (common set) of genes between all samples was high (~17 000 genes).

Fig. S3 Single-cell data from *Drosophila* embryos are reproducible and correlate well with bulk mRNAseq data. Related to Fig. 3.

a Identification of cell barcodes associated with single-cell transcriptomes for single-cell libraries from Drosophila embryos, a complex primary tissue harboring small, low RNA content cells. (For methods details, see Suppl. Fig. S1a.) Four of seven replicates are shown.

b Correlations between gene expression measurements from bulk mRNA-seq and 7 Drop-seq runs with methanol-fixed single cells (expressing >1000 UMIs) . Cells were from two independent biological samples representing dissociated *Drosophila* embryos (75% stages 10 and 11). Bulk mRNAseq data were generated with total RNA extracted directly from whole, intact, live embryos. (Sample 1: rep 1-2, rep 7 and bulk1; sample 2: rep 3-6 and bulk 2). Non-single cell bulk mRNA-seq data were expressed as reads per kilobase per million (RPKM). Drop-seq expression counts were converted to average transcripts per million (ATPM) and plotted as log2 (ATPM + 1). Upper right panel depicts Pearson correlations. The intersection (common set) of genes between all samples was high (~10 000 genes).

Fig. S4 Variance in single-cell data from *Drosophila* embryos and 2D cluster representations of replicates. Related to Fig. 3.

a Plots of principal components 1-30 of the 4 873 cell transcriptomes show variance captured in many principal components. Colors correspond to tSNE plot in Fig. 3b.

b 2D representation of experimental replicates in each cell population. tSNE plot from Fig. 3b with cells now colored by experimental Drop-seq replicate (left) or biological replicate sample (right). Clusters are formed by cells from many Drop-seq different runs (left) and from both samples (right).

The relatively more homogenous composition of cluster 8 (neurons) and 15 (LVM) is consistent with a higher proportion of embryos of later stages in sample 2.

Fig. S5 Single-cell data from mouse hindbrain are reproducible and correlate well with bulk mRNAseq data. Related to Fig. 4.

a Identification of cell barcodes associated with single-cell transcriptomes for single-cell libraries from FACS-sorted, fixed mouse hindbrain cells. (For methods details, see Suppl. Fig. S1.)

b Correlations between gene expression measurements from independent Drop-seq experiments with FACS-sorted methanol-fixed single cells (expressing >300 UMIs). Cells were from independent biological samples, representing dissected, dissociated mouse hindbrains and cerebellum from newborn mice. Bulk mRNAseq data were generated with total RNA extracted from cells after FACS and fixation. Non-single cell bulk mRNA-seq data were expressed as reads per kilobase per million (RPKM). Drop-seq expression counts were converted to average transcripts per million (ATPM) and plotted as log2 (ATPM + 1). Upper right panel depicts Pearson correlations. The intersection (common set) of genes between samples was ~17 000 genes.

Fig. S6 Variance in single-cell data from newborn mouse hindbrain and cerebellum and 2D cluster representation of replicates. Related to Fig. 4.

a Plots of principal components 1-18 of the 4 366 cell transcriptomes show variance in many principal components. Colors correspond to tSNE plot in Fig. 4b.

b 2D representation of experimental replicates in each cell population. tSNE plot from Fig. 4b with each cell now colored by experimental replicate. Note that cells from the two biological replicates are unevenly represented in the different clusters, likely reflecting dissection differences and, therefore, varying proportions of hindbrain to cerebellar tissue.

c We identified a subtype of myelinating glia, probably Schwann cells from cranial nerves entering the hindbrain (cluster 11, Fig. 4b). These cells express Myelin protein zero (*Mpz*) and other genes for myelin formation (Proteolipid protein 1, *Plp1*) and *Mbp* (Fig. 4b), but do not express oligodendrocyte markers such as *Bcas1* or *Olig1* (Fig. 4b).

Suppl. Figure S1

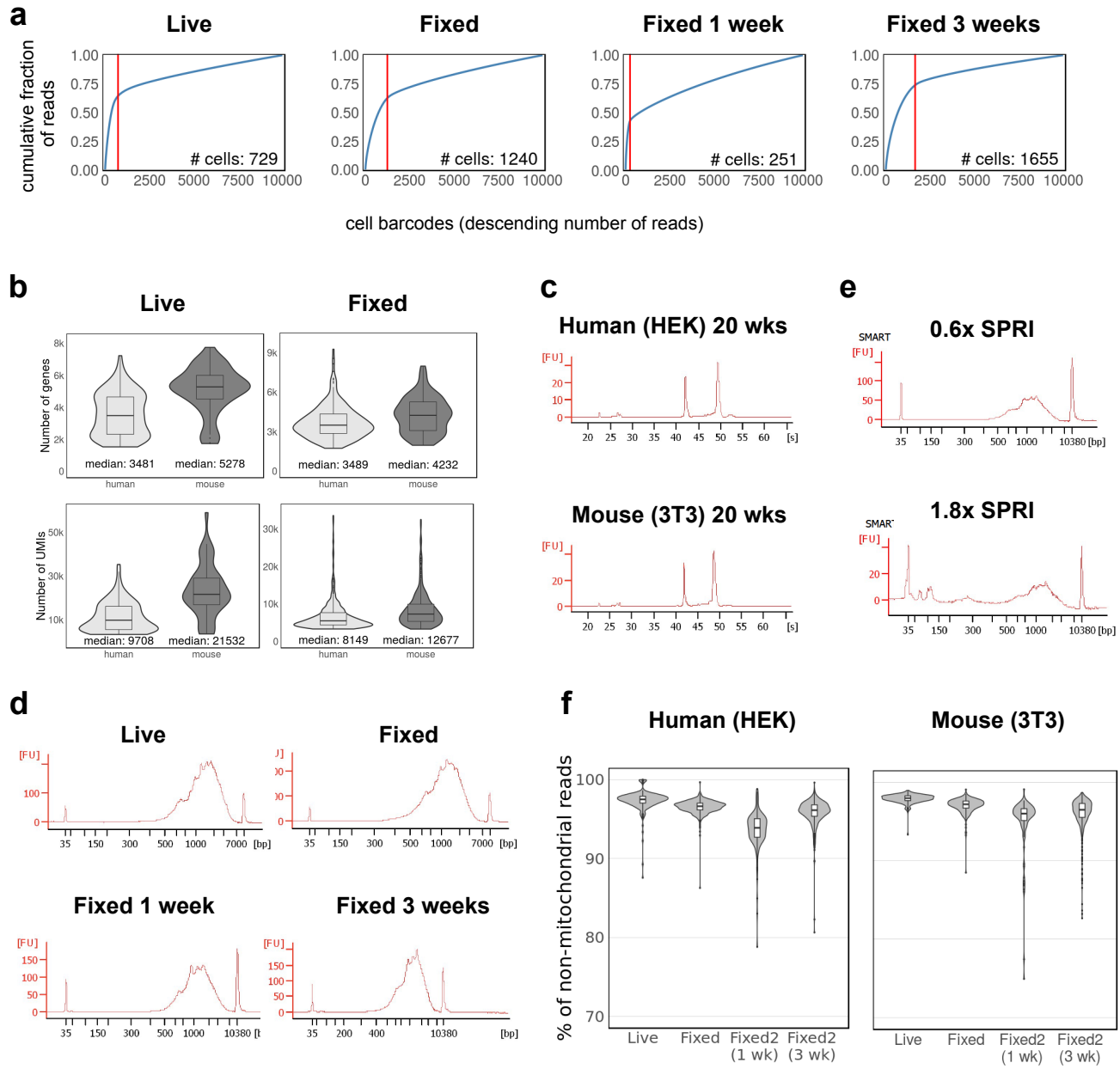

Suppl. Figure S2

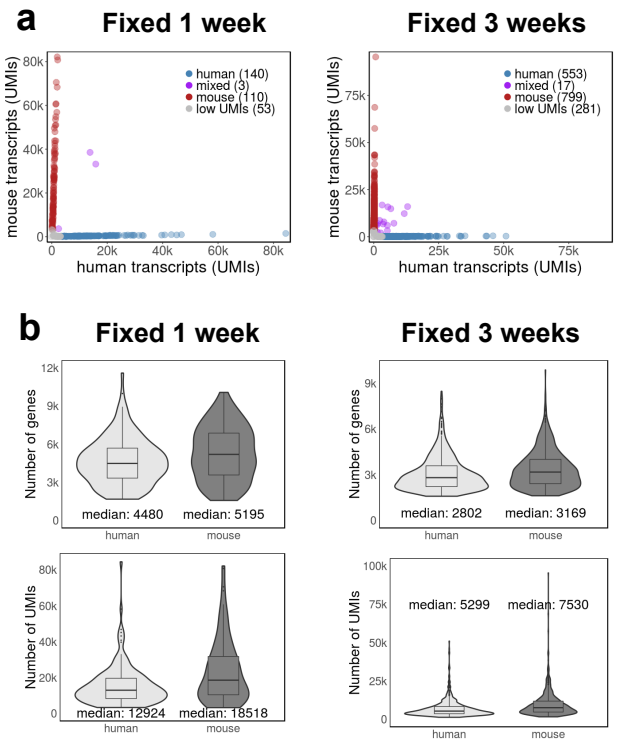

Suppl. Figure S3

a

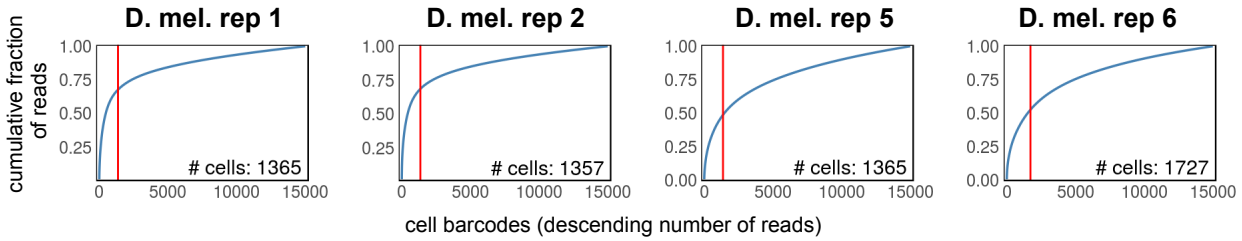

b

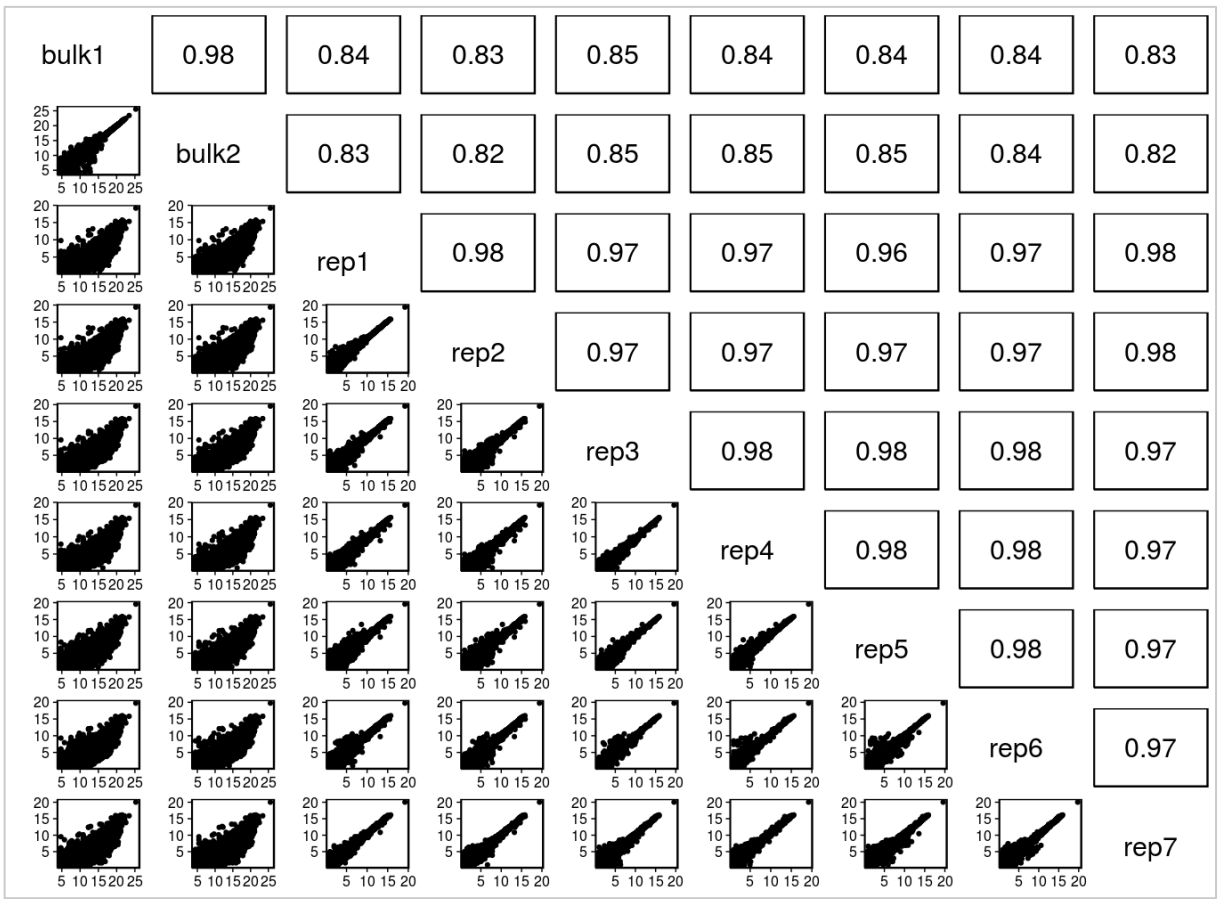

Suppl. Figure S4

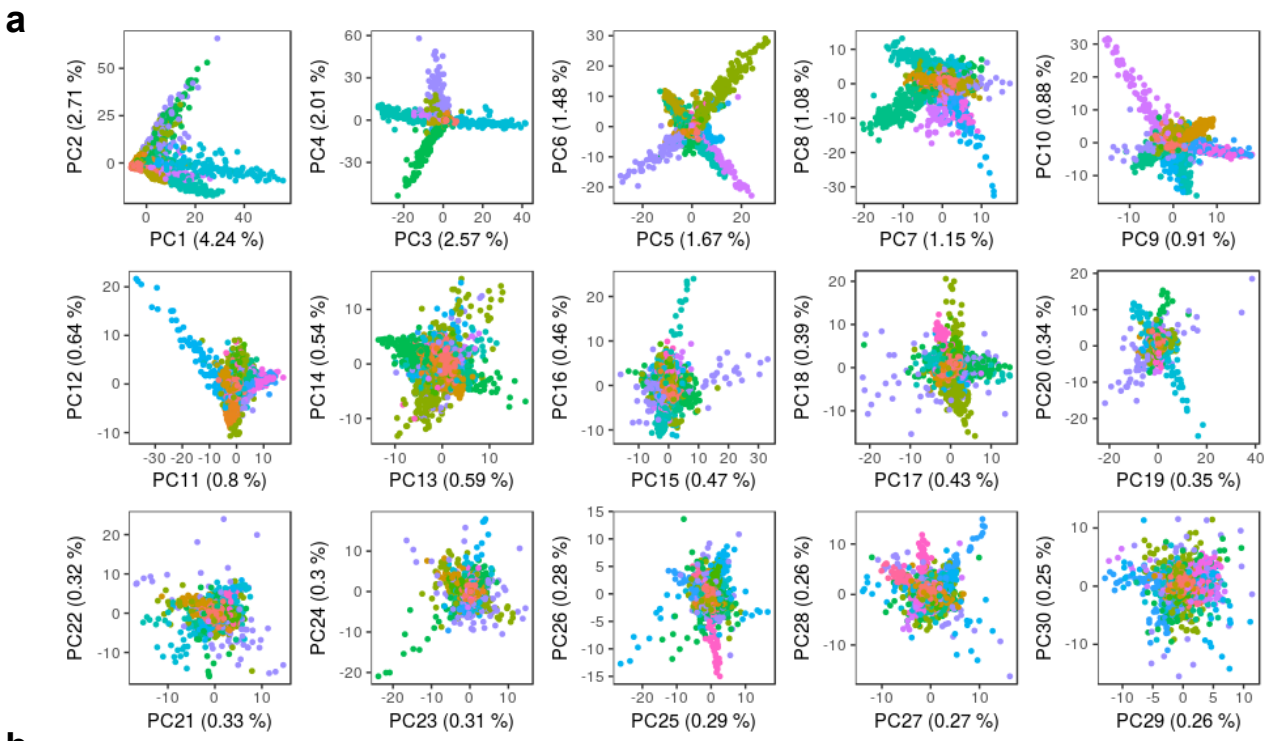

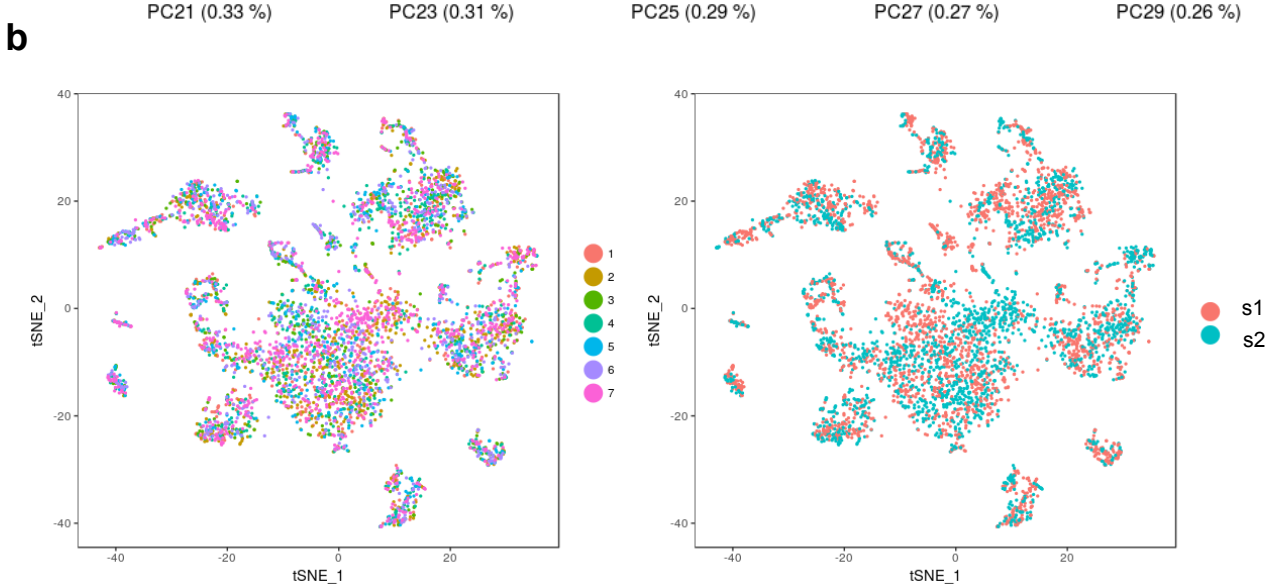

Suppl. Figure S5

a

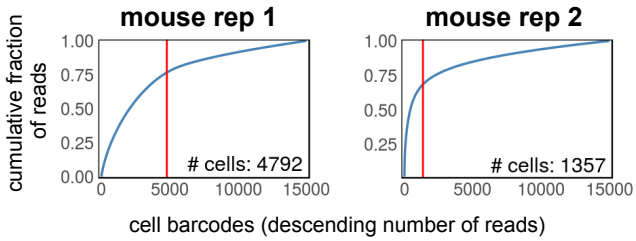

b

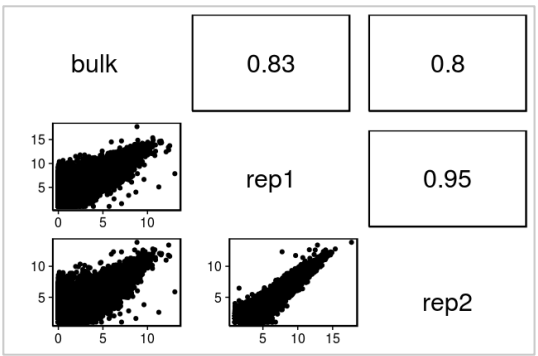

Suppl. Figure S6